ISSN 0036-0244, Russian Journal of Physical Chemistry A, 2022, Vol. 96, No. 4, pp. 765–772. © Pleiades Publishing, Ltd., 2022.
Russian Text © The Author(s), 2022, published in Zhurnal Fizicheskoi Khimii, 2022, Vol. 96, No. 4, pp. 553–561.

ON THE 90th ANNIVERSARY OF THE BIRTH OF G.A. KRESTOV

Conformational Equilibria of a Thiadiazole Derivative in Solvents of Different Polarities: an NMR Study

I. A. Khodov[a],*, K. V. Belov[a], M. A. Krestyaninov[a], and M. G. Kiselev[a]

[a] *Krestov Institute of Solution Chemistry, Russian Academy of Sciences, Ivanovo, 153045 Russia*

**e-mail: iakh@isc-ras.ru*

Received October 13, 2021; revised October 13, 2021; accepted October 14, 2021

Abstract—The spatial structure of the 1-[5-(4-methoxyphenylamino)-1,2,4-thiadiazol-3-yl]-propan-2-ol molecule is analyzed by the methods of nuclear magnetic resonance (NMR) spectroscopy and quantum chemical calculations using the density functional theory. The ratio of probable conformers of the compound in chloroform-d_1 and dimethylsulfoxide-d_6 is found. Conformational inversion of the compound molecules is observed upon changing the solvent.

Keywords: thiadiazole, spatial structure, conformers, NMR, NOESY

DOI: 10.1134/S0036024422040148

INTRODUCTION

Many compounds containing a five-membered heterocyclic ring have unique chemical properties and diverse biological activity types. Thiadiazole is considered a bioisostere of pyrimidine and oxadiazole [1].

Until recently, a thiadiazole fragment was a structural component in the synthesis of antiparasitic and antimicrobial drugs, some of which are still used in clinical practice [2]. Over the last decade, studies have shown that compounds containing a thiadiazole ring in their structure possess antitumor, antibacterial, anticonvulsant, and anti-inflammatory properties [3].

The aim of this work was to determine the spatial structure parameters and the proportion of conformers of 1-[5-(4-methoxyphenylamino)-1,2,4-thiadiazol-3-yl]-propan-2-ol, a thiadiazole derivative, in solvents of different polarities ($CDCl_3$ and DMSO-d_6). As it was shown in recent works, nuclear magnetic resonance (NMR) spectroscopy and nuclear Overhauser effect (NOE) spectroscopy in particular are convenient ways of solving such problems [4–8]. Our approach is based on determining the internuclear distances in the structure of a molecule based on cross relaxation rates obtained by analyzing the integral intensities of the signals in $^1H-^1H$ NOESY spectra.

EXPERIMENTAL

All the NMR experiments were performed on a Bruker Avance III 500 spectrometer. The operating frequencies for the ^1H and ^{13}C nuclei were 500.17 and 125.77 MHz, respectively. The temperature was controlled with a Bruker Temperature Control Unit (BVT-2000) combined with a Bruker Cooling Unit (BCU 05). The ^1H NMR spectra were obtained with a pulse sequence generated by TopSpin 3.6.1 spectrometer software. The number of scans was 128. The spectral range was 7500.00 Hz, the receiver gain coefficient (RG) was 6.4, and the number of points (TD) was 16384 [9].

Proton decoupled ^{13}C NMR spectra were also obtained with a pulse sequence generated by TopSpin 3.6.1 spectrometer software. The number of scans was 1024. The spectral range was 34722.22 Hz, the receiver gain was set automatically (256), and the number of points (TD) was 65536 [10].

A "noesygpphpp" pulse program was used to register the 2D NOESY NMR spectra. It generates a sequence consisting of three 90° RF pulses separated by a delay d_0 between the first and second pulses, a mixing time delay d_8 between the second and third pulses, and the time of free induction decay generation. The period of mixing d_8 for the NOESY experiments was from 0.1 to 0.9 s with a step of 0.1 s. The number of scans (NS) was 16. The spectral range was 7500.00 Hz along both axes. The relaxation period ($5T_1$) was chosen according to the recommendations for NMR experiments: 3 s [11–23].

Homo- and heteronuclear spectra ($^1H-^{13}C$ HSQC, $^1H-^{13}C$ HMBC, and $^1H-^1H$ TOCSY) were obtained using parameters found from 1D experiments (^1H and ^{13}C) [9, 24–31].

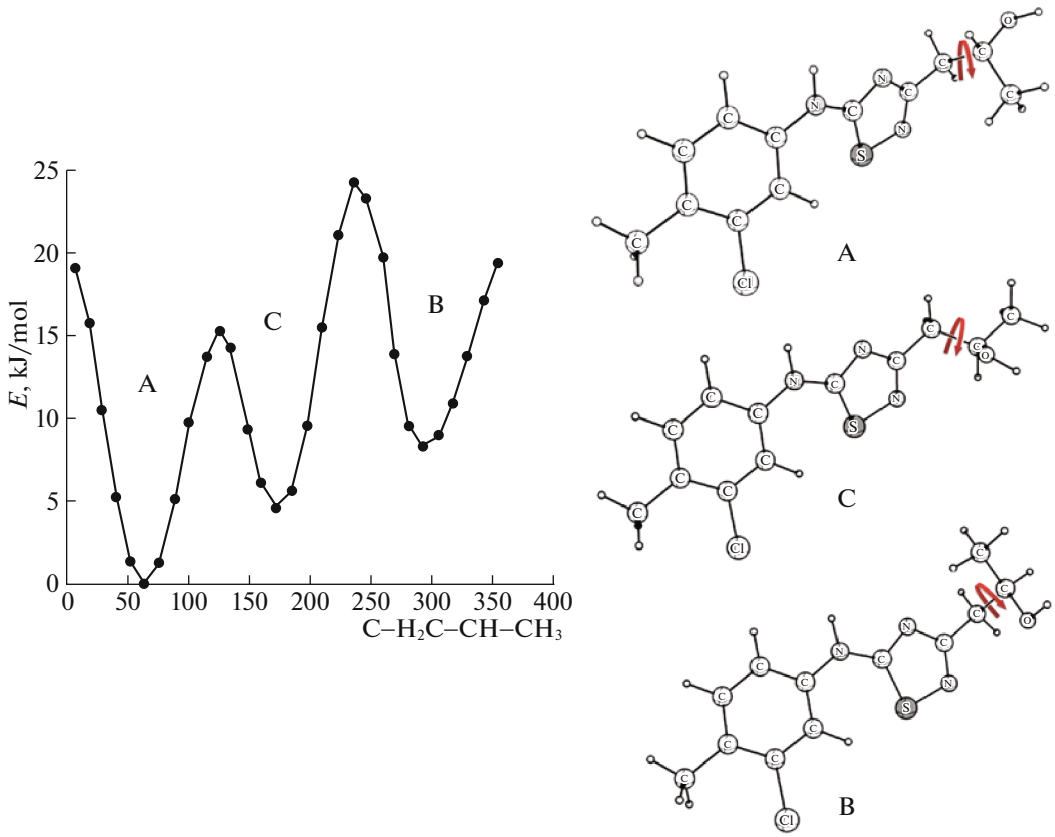

Fig. 1. Barriers to intramolecular rotation around the $H_2C–CH$ bond (τ_2) in the isopropanol fragment of the thiadiazole derivative molecule.

Quantum-chemical calculations were made using the Gaussian 16 software with an APFD DFT functional that included dispersion correction, in combination with a 6-311++G (2*d*,2*p*) basis set.

RESULTS AND DISCUSSION

A molecule of the thiadiazole derivative has five dihedral angles. Changes in these angles result in the formation of a variety of conformers conformers, including those with an intramolecular O–H···N hydrogen bond. The structures of 104 conformers were optimized. Twenty-eight conformers with intramolecular H-bonds had the lowest energies of those calculated. The remainder had no intramolecular hydrogen bonds. The mutual arrangement of two cyclic fragments that can either lie in the same plane or be displaced relative to each other also affects the formation of additional conformers of the thiadiazole derivative molecule. The vibrational spectra of the conformers were therefore calculated using quantum chemistry. None of the structures had imaginary frequencies.

Signals attributed to the conformers, in which the $H_2C–CH$ bond in the isopropanol side fragment is mobile, were observed in the NOESY spectrum. It was difficult to observe other conformers by NOESY, since the conformational distances that characterize the rotation of the remaining fragments of the molecules were beyond the method sensitivity (>5 Å).

Figure 1 shows the barriers to the intramolecular rotation around the $H_2C–CH$ (τ_2) bond in the isopropanol fragment without intramolecular hydrogen bonds, which enables such structural variety. The difference between the energy barriers is due to the CH_3 and OH groups. The O–H···N hydrogen bonds with the heterocycle nitrogen atoms hinder this rotation and can alter the energy barriers. Solvents capable of forming hydrogen bonds with an OH group (proton acceptors) or with N atoms (proton donors) can break the intramolecular N···H–O bond in the thiadiazole derivative molecule and change the isopropanol fragment conformation.

Nine resonance signals (Fig. 2) are observed in the ^1H NMR spectrum of 1-[5-(4-methoxyphenylamino)-1,2,4-thiadiazol-3-yl]-propan-2-ol (a thiadiazole derivative) in chloroform-d_1. The four resonance signals detected at 1.32 (d, H11), 2.39 (s, H12), 2.85 (dd, H9b), and 3.00 ppm (dd, H9a) are attributed to the CH_3 (H11 and H12) and CH_2 (H9a and H9b) groups of the molecule. The signals attributed to the

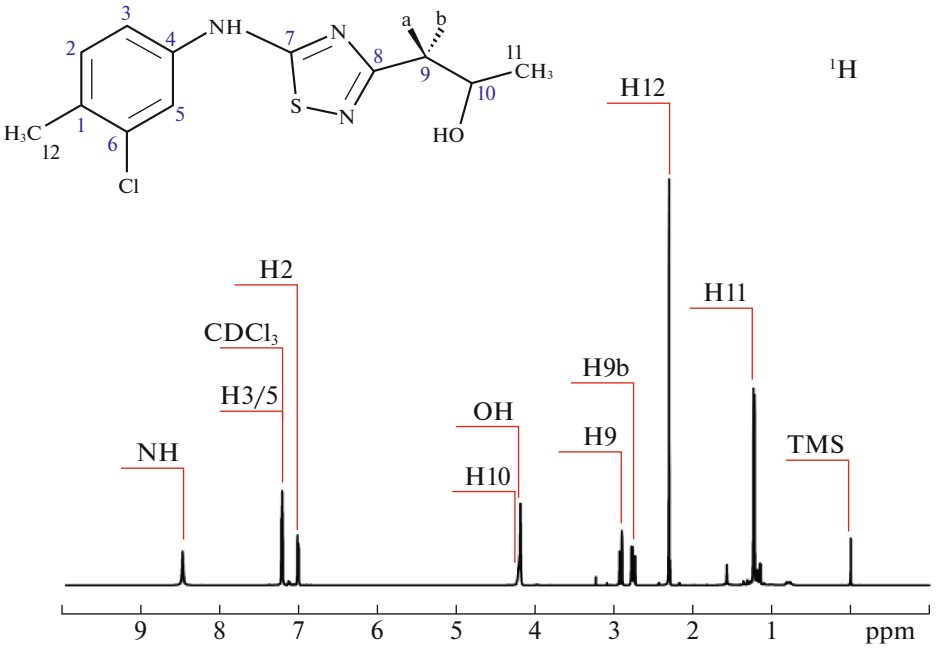

Fig. 2. ^{1}H NMR spectrum (500 MHz) of the thiadiazole derivative in chloroform-d_1.

CH, OH, and NH groups of the molecule are located at 4.27 (m, H10), 7.08 (dd, H2), 7.28 (dd, H3/5), 4.29 (s, OH), and 8.54 (s, NH) ppm. The unambiguous assignment of the resonance signals was made based on the 2D NMR, published data, and the shape of the characteristic group signals.

When the spatial structure of the thiadiazole derivative molecule was studied and the proportion of conformers was found, nuclear Overhauser effect spectra (^{1}H–^{1}H NOESY) were obtained with different mixing times. Figure 3 shows a NOESY spectrum with a mixing time of 0.9 s. It contains 14 pairs of cross peaks: H2–H11, H3/5–H11, H10–H2, H10–H3/5, H10–H9a, H10–H9b, H10–H11, H11–H9b, H11–H9a, H12–H3/5, NH–H3/5, NH–H2, NH–H10, and NH–H11 corresponding to the interactions between the hydrogen atoms. Further analysis of the integrated intensities of the cross peaks in the NOESY spectra responsible for the conformational and reference distances allowed us to calculate the populations of thiadiazole derivative conformers in the chloroform-d_1 solution with high accuracy.

Table 1 shows the chemical shifts of the signals in our 1D spectra and data on the intramolecular interactions found by analyzing the two-dimensional NMR spectra.

The test compound conformations in a solvent of different polarity were analyzed at the next stage. Nine resonance signals were observed in the ^{1}H NMR spectrum of the thiadiazole derivative in DMSO-d_6 (Fig. 4). The four resonance signals located at 1.17 (d, H11), 2.22 (s, H12), 2.75 (dd, H9b), and 2.89 ppm (dd, H9a) were attributed to the CH_3 (H11 and H12) and CH_2 (H9a and H9b) groups of the molecule. The signals at 4 to 9 ppm were attributed to the CH– (4.23 ppm, m, H10), 7.28 ppm (dd, H2), 7.21 ppm (dd, H3), 7.72 ppm (dd, H5), 4.79 ppm (s, OH), and 10.77 ppm (s, NH) groups of the molecule. The unambiguous assignment of the resonance signals was made based on the 2D NMR, published data, and the shape of the characteristic group signals.

Nuclear Overhauser effect spectra (^{1}H–^{1}H NOESY) were obtained to determine the spatial structure of the thiadiazole derivative molecule, calculate the interproton distances and the fractions the fractions of the conformers. Figure 5 shows a NOESY spectrum with a mixing time of 0.9 s. It contains six pairs of cross-peaks (H3–H12, H10–H9b, H10–H9a, H10–H11, H9a–H11, and H9b–H11) corresponding to the H–H interactions. Further analysis of the integrated intensities of the cross peaks in the NOESY spectra responsible for the conformational and reference distances allowed us to calculate the percentage of thiadiazole derivative conformers in the DMSO-d_6 solution with high accuracy.

Table 2 presents data on the chemical shifts in the 1D spectra and intramolecular interactions of the H–H and H–C types obtained by analyzing the 2D spectra.

The H10–H11 and H9a–H10 distances were used as the references to determine the other correlations between the hydrogen atoms (H2–H11, H3/5–H11, H10–H2, H10–H3/5, H10–H9a, H10–H9b, H10–H11, H11–H9b, H11–H9a, H12–H3/5, NH–H3/5, NH–H2, NH–H10, and NH–H11) observed in the

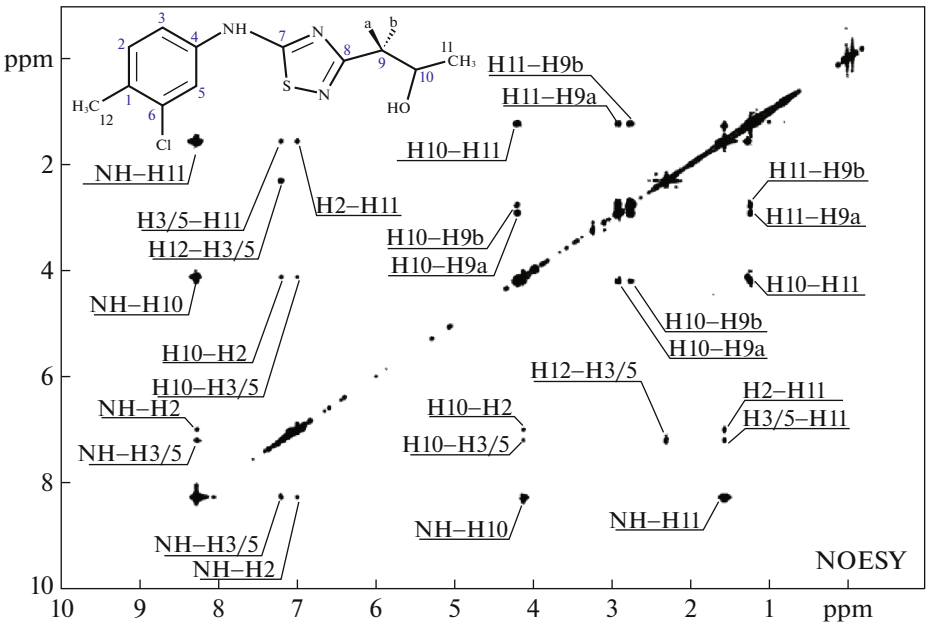

Fig. 3. ^{1}H–^{1}H NOESY spectrum of the thiadiazole derivative in chloroform-d_1.

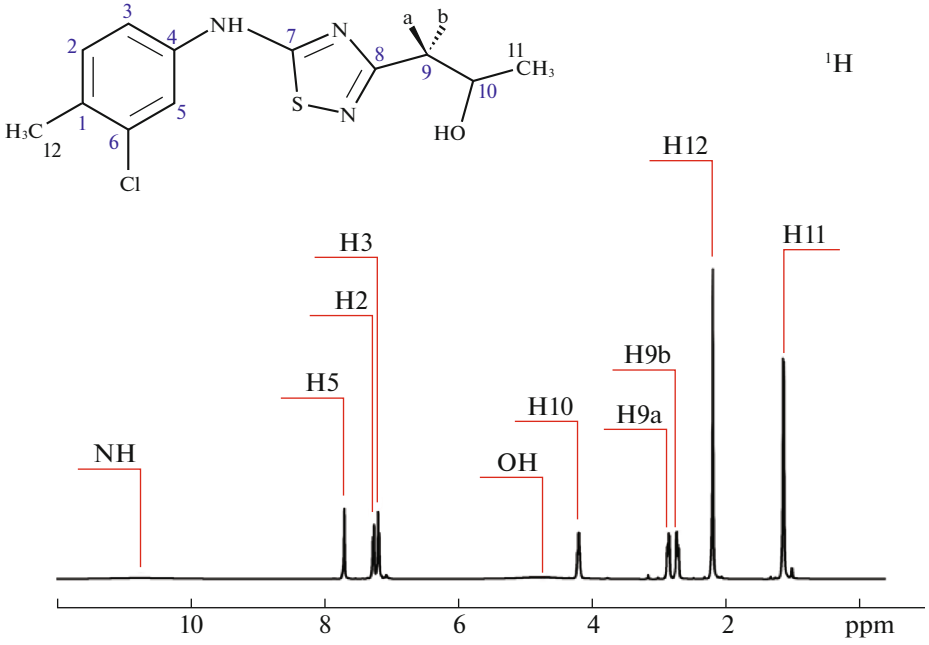

Fig. 4. ^{1}H NMR spectrum (500 MHz) of the thiadiazole derivative in DMSO-d_6.

NOESY experiment. Analysis of the conformer structure indicates that the reference distances are virtually independent of the molecule conformation to a tolerance of ±0.007 Å.

Since the analysis of the barriers to the intramolecular rotation in quantum-chemical calculations shows that there are three stable conformers due to the mobile isopropanol fragment of the molecule and since the conformation-determined distances of conformers A and C are similar within the experimental error, they are considered as one conformer in this work. As a result, the H9a–H10 distances are 3.04 Å for conformer A and 2.47 Å for B. The distances between these nuclei were obtained by analyzing the structure calculated by quantum chemistry, with the reference distance of 2.60 Å.

Table 1. ^{1}H and ^{13}C NMR chemical shifts and cross-correlation peaks in 2D spectra of the thiadiazole derivative in chloroform-d_1

δ ^{13}C, ppm	^{1}H	δ ^{1}H, ppm	HSQC	HMBC	TOCSY			NOESY	^{13}C
					20 ms	60 ms	100 ms		
132.17	—	—	—	C1–H12	—	—	—	—	C1
116.66	H2	7.08	C2–H2	—	—	—	—	H2–H11	C2
131.44	H3/5	7.28	C3–H3/5	C3–H12	H3/5–H2	H3/5–H2	H3/5–H2	H3/5–H11	C3
137.33	—	—	—	C4–H12	—	—	—	—	C4
119.25	–	–	C5–H3/5	C5–H12	—	—	—	—	C5
134.93	—	—	—	C6–H12	—	—	—	—	C6
180.34	—	—	—	—	—	—	—	—	C7
170.81	—	—	—	C8–H9b	—	—	—	—	C8
41.02	H9a	3.00	C9–H9a	C9–H11	H9a–H11 H9b–H11	H9a–H11 H9b–H11	H9a–H11 H9b–H11	—	C9
	H9b	2.85	C9–H9b						
65.56	H10	4.29	C10–H10	C10–H9b C10–H11	H10–H9b H10–H9a H10–H11	H10–H9b H10–H9a H10–H11	H10–H9b H10–H9a H10–H11	H10–H2 H10–H3/5 H10–H9a H10–H9b H10–H11	C10
22.19	H11	1.32	C11–H11	C11–H9b	—	—	—	H11–H9b H11–H9a	C11
19.00	H12	2.39	C12–H12	—	—	H12–H2 H12–H3/5	H12–H2 H12–H3/5	H12–H3/5	C12
—	OH	4.27	—	—	OH–H9b	OH–H9b	OH–H9b	—	—
—	NH	8.54	—	—	—	—	—	NH–H3/5 NH–H2 NH–H10 NH–H11	—
76.53	$CDCl_3$	7.29	—	—	—	—	—	—	

The relationships between the average integrated intensities of the cross peaks and the period of mixing were plotted after analyzing the NOESY data, and the cross-relaxation peaks were found. They were 0.0209 ± 0.0005, 0.0207 ± 0.0005, and 0.0111 ± 0.0006 for the H9a–H10 and 0.0187 ± 0.0020 for the H10–H11 distances in the thiadiazole derivative structure in chloroform-d_1 and DMSO-d_6, respectively. The experimental values were found using a spin pair model: 2.51 ± 0.04, 2.60 ± 0.04, 2.84 ± 0.04, and 2.60 ± 0.04 Å for the H9a–H10, H10–H11, and H11–H9a distances in the thiadiazole derivative structure in chloroform-d_1 and DMSO-d_6, respectively.

The dependences of the difference between the calculated and experimental conformation-dependent distances and the proportions of the conformers (Fig. 6, red and blue lines) were obtained along with the error in determining the experimental distance (dashed line) using a two-position exchange equation. The minima of the values on the graphs correspond to the most probable proportions of conformers, and the point where the lines intersect determines the error value. The results are shown on the diagrams.

Figure 7a shows the ratio of the most probable conformers of the thiadiazole derivative in chloroform and Fig. 7b presents the respective ratio in DMSO in DMSO. An analysis of the dependences indicates that the ratio of conformers A and B varies considerably due to the change in angle τ_2. Conformer B predominates in chloroform relative to A, with 61.9% of con-

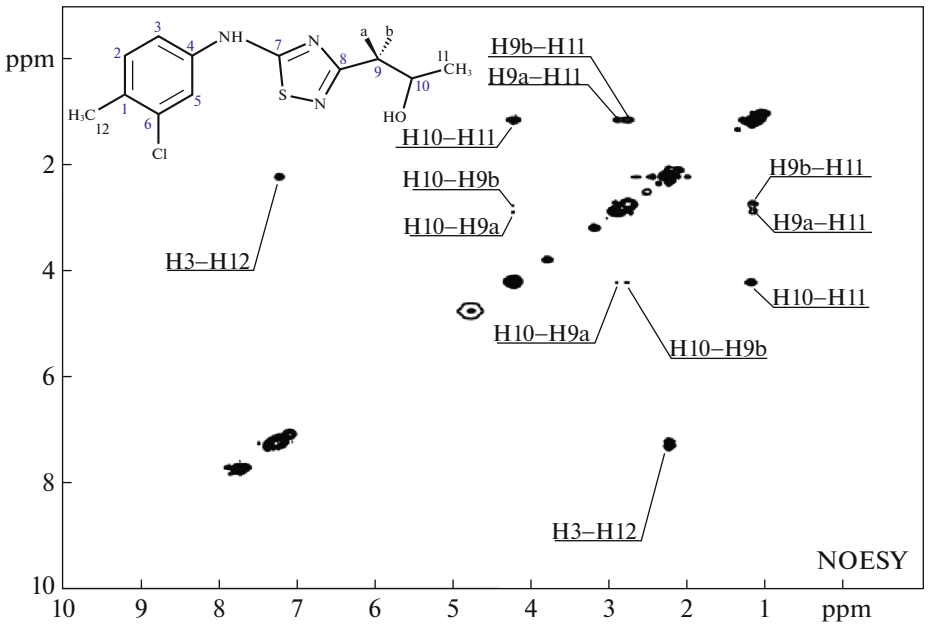

Fig. 5. ^{1}H–^{1}H NOESY spectrum of the thiadiazole derivative in DMSO-d_6.

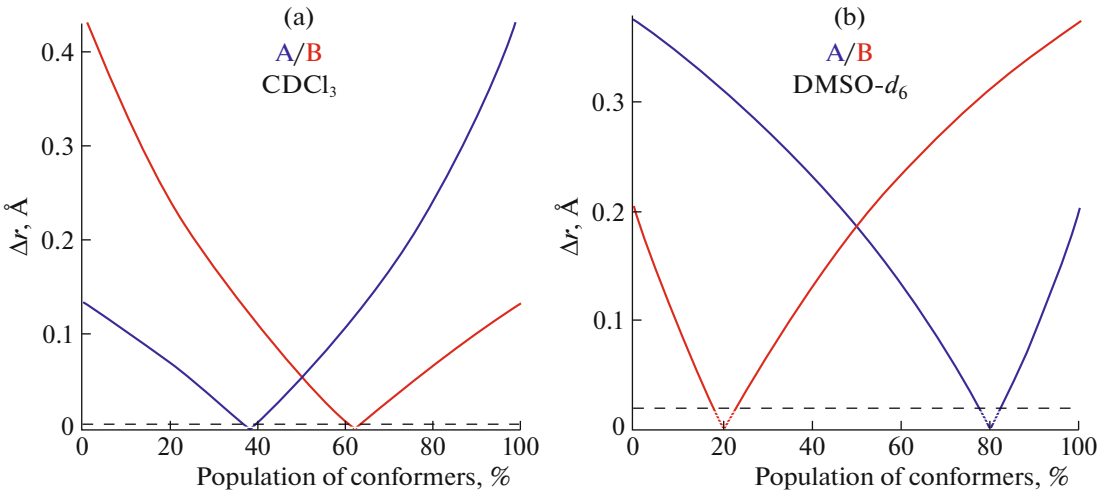

Fig. 6. Plot of average calculation error due to fitting the distribution of populations of conformers of thiadiazole derivative in (a) chloroform-d_1 and (b) DMSO-d_6 to experimental interproton distances (H9a–H10) obtained from 2D NOESY. The dashed line corresponds to the experimental distance error.

former B to 38.1% for conformer A (Fig. 7a). However, the situation is reversed in DMSO (Fig. 7b), where the ratio is 79% (conformer A) to 20.2 % (conformer B).

This result is similar to the one obtained for hydrazone derivatives (PLP-2FH and PLP-T2CH) and felodipine [6, 32], when the conformational inversion was observed upon the change in the concentration or chemical structure of the molecules. The intramolecular hydrogen bonds that form due to the differences in polymorphic solvates [33–35] play an important role, and the geometry of the molecules of both polymorphs differs in the terminal para-hydroxyl groups, in contrast to hydrazone and felodipine when considering changes in conformers. This effect is based on a mechanism with conformational polymorphism, referred to as solvatomorphism. The produced by the solid phase through the formation of a crystal solvate is therefore also typical of the thiadiazole derivative.

CONCLUSIONS

The proportions of conformers of a 1-[5-(4-methoxyphenylamino)-1,2,4-thiadiazol-3-yl]-propan-2-ol molecule resulting from the mobility of its isopro-

Table 2. ^{1}H and ^{13}C NMR chemical shifts and cross-correlation peaks in 2D spectra of the thiadiazole derivative in DMSO-d_6

δ ^{13}C, ppm	^{1}H	δ ^{1}H, ppm	HMBC	HSQC	TOCSY			NOESY	^{13}C
					20 ms	60 ms	100 ms		
128.97	—	—	C1–H12	—	—	—	—	—	C1
115.98	H2	7.28	—	C2–H2	H2–H3	H2–H3 H2–H12	H2–H3 H2–H12	—	C2
131.31	H3	7.21	C3–H12	C3–H3	—	H3–H12	H3–H12	H3–H12	C3
139.00	—	—	C4–H3	—	—	—	—	—	C4
117.56	H5	7.72	—	C5–H5	H5–H2 H5–H3	H5–H2 H5–H3	H5–H2 H5–H3	—	C5
133.54	—	—	C6–H3 C6–H12	—	—	—	—	—	C6
178.41	—	—	—	—	—	—	—	—	C7
170.00	—	—	C8–H9a C8–H9b	—	—	—	—	—	C8
42.81	H9a	2.89	C9–H11	C9–H9a	—	—	—	—	C9
	H9b	2.75	—	C9–H9b	—	—	—		
65.30	H10	4.23	C10–H9a C10–H9b C10–H11	C10–H10	H10–H9b H10–H9a H10–H11	H10–H9b H10–H9a H10–H11	H10–H9b H10–H9a H10–H11	H10–H9b H10–H9a H10–H11	C10
23.23	H11	1.17	C11–H9a C11–H9b	C11–H11	H9a–H11 H9b–H11	H9a–H11 H9b–H11	H9a–H11 H9b–H11	H9a–H11 H9b–H11	C11
18.76	H12	2.22	C12–H3	C12–H12	—	—	—	—	C12
—	OH	4.79	—	—	—	—	—	—	—
—	NH	10.77	—	—	—	—	—	—	—
76.53	$CDCl_3$	7.28	—	—	—	—	—	—	
128.97	—	—		—	—	—	—	—	C1

panol fragment in tow solvents of different polarity were determined by nuclear Overhauser effect spectroscopy and quantum-chemical calculations. The conformational inversion was probably due to the so-called solvatomorphism. Our results can be used in the synthesis of new and modification of the existing

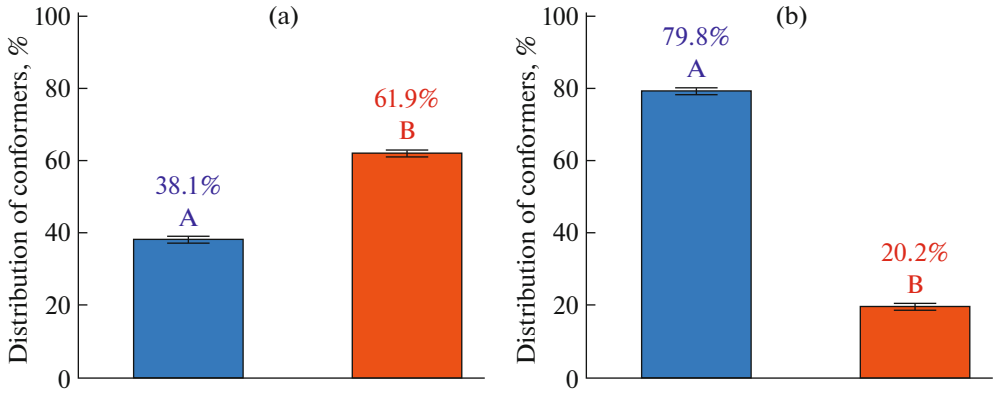

Fig. 7. Distribution of the thiadiazole molecule conformers in (a) chloroform-d_1 and (b) DMSO-d_6, based on experimental 2D NOESY data.

biologically active drugs based on thiadiazole derivatives.

FUNDING

This work was supported by the RF Ministry of Higher Education and Science, project nos. 01201260481 and 0120095082; the Russian Foundation for Basic Research, project nos. 18-29-06008 and 20-43-370011; and the RF Presidential Grant Council, project no. MK-662.2021.1.3.

ACKNOWLEDGMENTS

Our NMR experiments were performed on the equipment of the Krestov Institute of Solution Chemistry, Russian Academy of Sciences (http://www.ckp-rf.ru/usu/503933/).

REFERENCES

1. Y. Li, J. Geng, Y. Liu, et al., ChemMedChem **8**, 27 (2013).
2. Y. Hu, C.-Y. Li, X.-M. Wang, et al., Chem. Rev. Am. Chem. Soc. **114**, 5572 (2014).
3. B. Sharma, A. Verma, S. Prajapati, and U. K. Sharma, Int. J. Med. Chem. **2013**, 1 (2013).
4. I. A. Khodov, M. Y. Nikiforov, G. A. Alper, et al., J. Mol. Struct. **1035**, 358 (2013).
5. I. A. Khodov, S. V. Efimov, V. V. Klochkov, et al., Eur. J. Pharm. Sci. **65**, 65 (2014).
6. G. A. Gamov, I. A. Khodov, K. V. Belov, et al., J. Mol. Liq. **283**, 825 (2019).
7. K. V. Belov, I. E. Eremeev, V. V. Sobornova, et al., Macroheterocycles **13**, 44 (2020).
8. I. A. Khodov, K. V. Belov, A. E. Pogonin, et al., J. Mol. Liq. **342**, 117372 (2021).
9. M. Liu, X. A. Mao, C. Ye, et al., J. Magn. Reson. **132**, 125 (1998).
10. I. A. Khodov, K. V. Belov, S. V. Efimov, and L. A. E. B. de Carvalho, AIP Conf. Proc. **2063** (2019).
11. H. Kessler, H. Oschkinat, C. Griesinger, and W. Bermel, J. Magn. Reson. **70**, 106 (1986).
12. J. Stonehouse, P. Adell, A. J. Shaka, and J. Keeler, J. Am. Chem. Soc. **116**, 6037 (1994).
13. K. Stott, J. Keeler, T. L. Hwang, et al., J. Am. Chem. Soc. **117**, 4199 (1995).
14. M. J. Thrippleton and J. Keeler, Angew. Chem. Int. Ed. **42**, 3938 (2003).
15. S. A. Katkova, M. A. Kinzhalov, P. M. Tolstoy, et al., Organometallics **36**, 4145 (2017).
16. P. P. Kobchikova, S. V. Efimov, I. A. Khodov, and V. V. Klochkov, J. Mol. Liq. **336**, 116244 (2021).
17. S. I. Selivanov, S. Wang, A. S. Filatov, and A. V. Stepakov, Appl. Magn. Reson. **51**, 165 (2020).
18. S. I. Selivanov, Appl. Magn. Reson. **49**, 563 (2018).
19. A. S. Smirnov, A. S. Kritchenkov, N. A. Bokach, et al., Inorg. Chem. **54**, 11018 (2015).
20. I. Khodov, S. Efimov, M. Krestyaninov, et al., J. Pharm. Sci. **110**, 1533 (2021).
21. K. S. Usachev, A. V. Filippov, B. I. Khairutdinov, et al., J. Mol. Struct. **1076**, 518 (2014).
22. K. S. Usachev, A. V. Filippov, E. A. Filippova, et al., J. Mol. Struct. **1049**, 436 (2013).
23. L. F. Galiullina, H. A. Scheidt, D. Huster, et al., Biochim. Biophys. Acta **1861**, 584 (2019).
24. A. G. Palmer III, J. Cavanagh, P. E. Wright, and M. Rance, J. Magn. Reson. **93**, 151 (1991).
25. L. E. Kay, P. Keifer, and T. Saarinen, J. Am. Chem. Soc. **114**, 10663 (1992).
26. J. Schleucher, M. Schwendinger, M. Sattler, et al., J. Biomol. NMR **4**, 301 (1994).
27. D. O. Cicero, G. Barbato, and R. Bazzo, J. Magn. Reson. **148**, 209 (2001).
28. A. Bax and D. G. Davis, J. Magn. Reson. **65**, 355 (1985).
29. I. A. Khodov, M. G. Kiselev, S. V. Efimov, and V. V. Klochkov, J. Magn. Reson. **266**, 67 (2016).
30. P. A. Kalmykov, I. A. Khodov, V. V. Klochkov, and M. V. Klyuev, Russ. Chem. Bull. **66**, 70 (2017).
31. G. B. Guseva, E. V. Antina, and M. B. Berezin, ACS Appl. Biol. Mater. **4**, 6227 (2021).
32. I. A. Khodov, S. V. Efimov, M. Y. Nikiforov, et al., J. Pharm. Sci. **103**, 392 (2014).
33. A. A. Hoser, D. M. Kamiński, A. Matwijczuk, et al., CrystEngComm **15**, 1978 (2013).
34. A. A. Hoser, D. M. Kamiński, A. Skrzypek, et al., Cryst. Growth Des. **18**, 3851 (2018).
35. D. Karcz, A. Matwijczuk, B. Boroń, et al., J. Mol. Struct. **1128**, 44 (2017).

Translated by A. Tulyabaev